JOURNAL OF CATALYSIS **178,** 26–33 (1998)
ARTICLE NO. CA982115

Structure Sensitive Hydrogen Adsorption: Effect of Ag on Ru/SiO_2 Catalysts

N. Savargaonkar,*,† R. L. Narayan,*,† M. Pruski,† D. O. Uner,‡ and T. S. King*,†

*Department of Chemical Engineering, †Ames Laboratory, Iowa State University, Ames, Iowa 50011; and ‡Chemical Engineering, Middle East Technical University, Ankara 06531, Turkey

Received April 28, 1997; revised March 5, 1998; accepted April 21, 1998

The dynamics and energetics of hydrogen chemisorption on silica-supported ruthenium and ruthenium–silver bimetallic catalysts were studied by ^1H NMR spectroscopy and microcalorimetry. It was observed that the amount of hydrogen adsorbed on Ru particles having intermediate and low heats of adsorption was significantly reduced with increasing amounts of silver. The desorption and adsorption rate constants, determined from selective excitation NMR experiments, were lower on Ru–Ag catalysts than those on Ru catalysts at the same temperature and hydrogen coverage. The apparent sticking coefficients of hydrogen on a Ru–Ag catalyst with 10 at% Ag were more than 10 times lower than those on a Ru catalyst and were comparable to sticking coefficients reported in the literature for hydrogen adsorbing on Ru single crystal. Thus silver was found to greatly affect both the dynamics and energetics of hydrogen chemisorption on Ru/SiO_2. However, ensemble and electronic effects did not play any role in causing these effects. It is postulated here that the influence of silver was due to its tendency to selectively segregate to edge, corner, and other low coordination structures on the Ru particle surface. Hence, hydrogen adsorption on these surfaces was found to be structure sensitive.

INTRODUCTION

The addition of a second element to a transition metal catalyst can result in marked changes in surface properties, affecting its activity and selectivity for various reactions (1–4). In some cases it is desirable to add a less active metal such as Ag, Au, or Cu, in order to improve selectivity toward a desired product (5–7). Even though Ag is catalytically inert for many hydrocarbon reactions, it appears to modify the activity of Ru/SiO_2. For example, Smale and King (7) observed that the ethane hydrogenolysis activity (per surface ruthenium site) of $Ru–Ag/SiO_2$ catalysts was much lower than that of Ru/SiO_2 catalysts. They also observed that the order of the reaction with respect to hydrogen was more negative on Ru–Ag catalysts compared to supported Ru.

The modification of catalytic activity in the manner noted above is usually explained by invoking electronic and/or ensemble effects. Electronic effects refer to perturbations in the electronic properties of the two metals when they are brought into intimate contact. However, Rodriguez (8), using temperature-programmed desorption (TPD), X-ray photoelectron spectroscopy (XPS), and X-ray excited Auger electron spectroscopy (XAES), observed that a Ag monolayer on Ru(0001) did not introduce significant electronic perturbations in the Ru surface. Ensemble effects refer to variation in catalytic activity resulting from a change in the number of active sites composed of groups (ensembles) of contiguous, active metal atoms. Given the fact that Ru and Ag do not form miscible alloys because of their extreme clustering tendency, it is unlikely that an ensemble effect is operable. Indeed, the atomistic simulations (7, 9) indicated that Ag preferentially occupied edge, corner and other low metal coordination sites. Furthermore, ^1H NMR studies showed that at higher silver contents two- and three-dimensional Ag islands on Ru were formed with essentially no mixing of Ag and Ru atoms on the surface planes (10).

This view of the interaction of Ru and Ag is supported by the single crystal study of Schick *et al*. (11), who observed via photoemission of adsorbed xenon (PAX) and angle-resolved ultraviolet photoemission spectroscopy (ARUPS) that Ag preferentially occupied the step sites when deposited on a stepped Ru surface. The results indicated that Ag formed one-dimensional rows along the trough-like structures. The PAX results showed that Ag did form three-dimensional islands on a Ru(0001) surface. Hence both theory and experiment agree that reduction of Ru ensembles by the presence of Ag is not likely to occur. If both electronic and ensemble effects are discounted as potential explanations for the behavior of Ru–Ag catalysts, then other effects must be considered.

The objective of this work was to investigate the effects of silver addition on the hydrogen chemisorption behavior and mobility of hydrogen on Ru/SiO_2 and $Ag–Au/SiO_2$ catalysts by means of ^1H NMR and microcalorimetry. NMR is a quantitative technique, and selective excitation ^1H NMR is useful in studying hydrogen dynamics (adsorption, desorption, and surface mobility) relevant to

0021-9517/98 $25.00

understanding mechanisms of various hydrogenation and hydrogenolysis reactions (12). It is well known that Ag does not dissociatively adsorb molecular hydrogen but may adsorb atomic hydrogen at temperatures below about 195 K (13). Therefore, hydrogen does not spill over from Ru to Ag at room temperature or higher (10) unlike the Ru–Cu/SiO_2 system (14). Hence NMR was used to determine accurate hydrogen-on-metal isotherms, kinetic parameters of adsorption and desorption, and modification of the surface electronic properties of Ru. Microcalorimetry was employed in this work to give complementary information regarding the energetics of hydrogen adsorption as a function of hydrogen coverage and Ag content. It was found that electronic and ensemble effects were not responsible for affecting the dynamics and energetics of hydrogen on Ag–Ru/SiO_2. It is postulated here that the change in hydrogen mobility and chemisorption energetics associated with the presence of Ag on a supported-Ru surface is the result of Ag preferentially populating edge, corner, and other low metal coordination sites. That is, the kinetic processes of hydrogen adsorption are structure sensitive.

METHODS

Catalyst Preparation

All the supported catalysts used in this study had a Ru loading equal to 4% by weight of the total (Ru and SiO_2) content. A 4% Ru/SiO_2 catalyst was prepared from a 1.5% ruthenium nitrosyl nitrate solution [$Ru(NO)(NO_3)_3$, Strem Chemicals] and silica [Cab-O-Sil HS-5] using the incipient wetness impregnation method. A slurry was prepared by impregnating the silica support with an appropriate amount of solution. This slurry was dried overnight at room temperature and then at 383 K for 2 h. The catalysts were subsequently reduced in flowing hydrogen at 673 K. The $Ru–Ag/SiO_2$ catalysts were prepared by coimpregnation with addition of $AgNO_3$ and $Ru(NO)(NO_3)_3$. Ag contents given in Table 1 are reported as at% of the total metal (Ru + Ag) and as wt% of total weight ($Ru + Ag + SiO_2$).

TABLE 1

The Dispersions and the Zero Pressure Knight Shifts of Mono- and Bimetallic Catalysts

Ag (at%)	Ag (wt%)	Ru dispersion (%)	Knight shifts (at zero pressure)
0	0.0	$11. \pm 1$	-65 ± 1
3	0.13	6.3 ± 0.6	-70 ± 1
10	0.47	$12. \pm 1$	-68 ± 1
20	1.06	8.8 ± 1	-69 ± 3
30	1.79	7.6 ± 0.8	-65 ± 3

Note. All catalysts had a Ru loading of 4 wt%. At% Ag is the percentage of the metal (Ru + Ag) in the catalyst which is Ag. Similarly, wt% Ag is the fraction of the total catalyst weight ($Ru + Ag + SiO_2$) which is Ag.

Throughout this paper the bimetallic catalysts are labeled by the at% Ag. For example, a Ru–Ag catalyst with 10 at% Ag is called Ru–10Ag. All catalysts were washed 8 to 10 times with 60 ml hot water per gram of catalyst to eliminate Na and Cl contamination. Dispersions of the catalysts studied in this work (see Table 1) were determined using the optimized volumetric method and by ^{1}H NMR (15). In both approaches it was assumed that one hydrogen atom adsorbed on one surface Ru atom under conditions where only strongly bound hydrogen was present. Strongly bound hydrogen was characterized as the hydrogen that could not be desorbed during a 10-min evacuation period at room temperature.

^{1}H NMR

The NMR experiments employed a home-built spectrometer with a proton resonance frequency of 250 MHz. The measurements were done using a home-built *in situ* NMR probe connected to a vacuum/dosing manifold which allowed for easy control of hydrogen pressure and temperature during the measurements. The catalysts were reduced at 673 K for 2 h in the NMR probe with hydrogen gas every 30 min. Before recording the NMR spectra, hydrogen was dosed onto the sample and equilibrated for 10 min. All spectra were recorded at a temperature of either 304 ($\pm$1) or 400 ($\pm$1) K with a repetition time of 0.5 s. Selective excitation experiments were done using DANTE (delays alternating with nutations for tailored excitation) sequence consisting of 30 short pulses (12). A pulse separation of 20 μs was chosen to result in a total duration of the DANTE sequence of 600 μs and corresponding spectral excitation width of $\approx$1.7 kHz. The overall flip angle of the DANTE sequence was adjusted by varying the width of the short pulses while the rf amplitude remained constant. After a recovery period of 20 μs, a final 90° pulse was applied followed by the detection of the free induction decay.

Microcalorimetry

A home built Tian Calvet differential heat flux microcalorimeter based on the design of Handy *et al.* (16, 17) was used in this work. The catalyst was loaded in a thin-walled pyrex NMR tube (Wilmad Glass Co.) connected to a stainless steel volumetric system with greaseless fittings. Static reduction of the catalyst was carried out *in situ* with the hydrogen replenished every 30 min, followed by evacuation at the reduction temperature for a period of time equal to the total time of reduction. The samples were allowed to thermally equilibrate overnight in the calorimeter at 400 K. Differential heats of adsorption were measured at 400 K to ensure that adsorbed hydrogen had sufficient mobility to probe the energetics of the entire sample surface (18). This strategy is justified by previous NMR studies which

indicated that adsorbed hydrogen is highly mobile on Ru and through the system at this temperature (12).

RESULTS

^1H NMR

The samples examined by ^{1}H NMR spectroscopy include one Ru/SiO_2 and four $Ru–Ag/SiO_2$ catalysts with atomic loadings of 3, 10, 20, and 30% Ag. The spectra taken at 7 Torr H_2 for these five catalysts all contain two peaks (see Fig. 1). The downfield peak at around 3 ppm is due to the hydroxyl groups of the silica support and hydrogen spilled over from Ru particles onto the support (19–21). The upfield peak corresponds to hydrogen adsorbed on Ru particles and its large shift is due to the interaction of the proton spins with the metal conduction electrons (Knight shift). The Knight shifts for the various catalysts at 7 Torr H_2 were essentially the same around −70 ppm regardless of the Ag content. Similarly, the Knight shifts obtained by extrapolating to zero hydrogen pressure, given in Table 1, were around −68 ppm and did not vary significantly with the Ag content.

As we mentioned earlier, Ag can block Ru adsorption sites, but it does not adsorb hydrogen or accommodate hydrogen atoms that could spillover from adjacent Ru atoms (10). Thus, the ratios of hydrogen to surface ruthenium, $H/Ru_{surface}$ (see Fig. 2), could be easily determined from the NMR spectra taken at 400 K and using the Ru loading and dispersion values from Table 1. Note that the dispersions of the catalysts were determined in experiments that differed from the experiments in which the isotherms shown in Fig. 2 were determined. They are in approximate agreement as noted by the ratio approaching the value of one at low pressures. The isotherms will go to zero coverage if the experiments are allowed to equilibrate at pressures approaching zero (less than 10^{-3} Torr). The intensity of the hydrogen-on-metal resonance represents hydrogen on the surface of Ru plus the gas phase hydrogen, because gaseous and surface hydrogen are in fast exchange on the NMR time scale (12). The $H/Ru_{surface}$ values were obtained after subtracting the contribution from the gas phase hydrogen from the total intensity. The amount of gas phase hydrogen was calculated to be about 30% of the total signal at 700 Torr. It can be seen from Fig. 2 that $H/Ru_{surface}$ is reduced with increasing amounts of Ag.

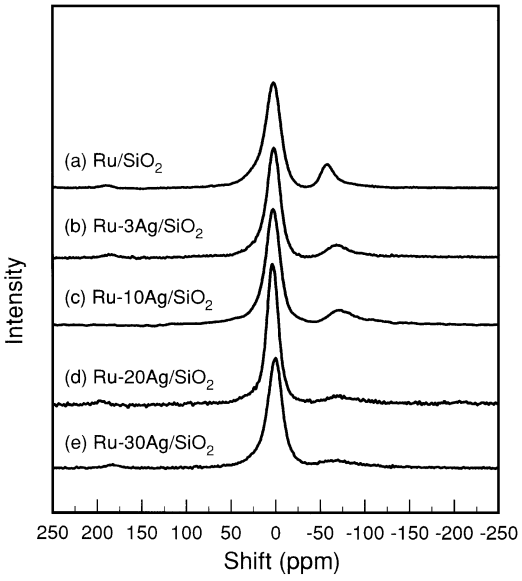

FIG. 1. ^{1}H NMR spectra for SiO_2-supported Ru and Ru−Ag catalysts at 7 Torr H_2. The Ru weight loading is 4% on all catalysts and the at% of Ag in each catalyst is indicated.

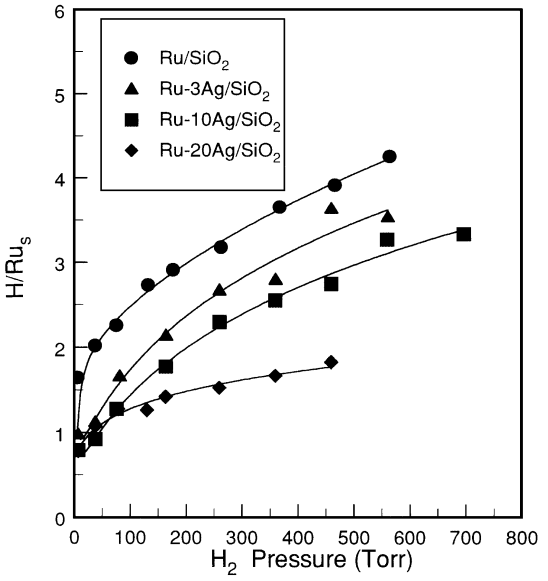

FIG. 2. Hydrogen adsorption isotherms determined via ^{1}H NMR at 400 K for Ru/SiO_2 and $Ru–3Ag/SiO_2$, $Ru–10Ag/SiO_2$, and $Ru–20Ag/SiO_2$.

At low hydrogen coverages, the NMR line due to H on Ru was inhomogeneously broadened, and selective inversion of part of this hydrogen population was achieved by applying the DANTE pulse sequence. The exchange parameters for interparticle hydrogen motion were determined by comparing the observed selective excitation spectra with simulated spectra obtained from a multisite exchange model developed by Engelke *et al.* (12). The model assumed that hydrogen desorption was a pseudo-first-order process. The adsorption and desorption rate constants estimated from the exchange parameters using this model are listed in Table 2. A plot of the desorption rate constant k_d versus $1/T$ at a hydrogen coverage of 0.4 is shown in Fig. 3 for both Ru/SiO_2 and $Ru–10Ag/SiO_2$. An activation energy of 52 ± 5 kJ/mol was obtained from this plot for the Ru–10Ag catalyst and a somewhat lower value of 43 ± 5 kJ/mol was obtained for Ru. Rate constants for adsorption were found to be insensitive to temperature and hence are not shown. Apparent sticking coefficients based on the entire Ru

TABLE 2

The Adsorption and Desorption Rate Constants for (top) Ru/SiO_2 Catalyst at 296 K and (bottom) $Ru{-}10Ag/SiO_2$ Catalyst at 296 K

H/Ru_s	0.42 ± 0.05	0.63 ± 0.06	0.73 ± 0.06	0.83 ± 0.08
k_d (s^{-1})	$4.8 \times 10^2 \pm 0.8 \times 10^2$	$7.9 \times 10^3 \pm 0.9 \times 10^3$	$2.1 \times 10^4 \pm 0.5 \times 10^4$	$2.4 \times 10^4 \pm 0.5 \times 10^4$
k_a (s^{-1} Pa^{-1})	$6.3 \times 10^2 \pm 1.2 \times 10^5$	$8.7 \times 10^2 \pm 1.0 \times 10^5$	$5.7 \times 10^2 \pm 1.4 \times 10^5$	$1.5 \times 10^5 \pm 0.3 \times 10^5$
H/Ru_s	0.42 ± 0.05	0.6 ± 0.06	0.76 ± 0.06	0.85 ± 0.08
k_d (s^{-1})	$1.9 \times 10^1 \pm 0.4 \times 10^1$	$1.0 \times 10^2 \pm 0.2 \times 10^2$	$3.9 \times 10^2 \pm 0.8 \times 10^2$	$1.2 \times 10^3 \pm 0.2 \times 10^3$
k_a (s^{-1} Pa^{-1})	$2.5 \times 10^4 \pm 0.5 \times 10^4$	$8.5 \times 10^3 \pm 1.7 \times 10^3$	$1.5 \times 10^4 \pm 0.3 \times 10^4$	$9.6 \times 10^3 \pm 1.5 \times 10^4$

surface were calculated using the desorption and adsorption rate constants (22) and are plotted in Fig. 4 for the Ru/SiO_2 and $Ru{-}10Ag/SiO_2$ catalysts. The sticking coefficients of hydrogen on Ru(0001) reported in the literature (23) are also included in Fig. 4 for comparison. The apparent sticking coefficients of hydrogen on the $Ru{-}Ag/SiO_2$ catalyst are similar to those on the single crystal Ru surface and are as much as 30 to 50 times lower than those on the Ru/SiO_2 catalyst at a given coverage.

Microcalorimetry

In Fig. 5 the differential heats of hydrogen adsorption on a series of $Ru{-}Au/SiO_2$ catalysts are shown as a function of hydrogen coverage expressed as $H/Ru_{surface}$. It was observed that adding Ag does not affect the initial heat of adsorption. However, Ag reduced the amount of hydrogen with intermediate (20 to 60 kJ/mol) and low (<20 kJ/mol) heats of adsorption, especially for the catalysts with 20 at% Ag or more. Interestingly, the catalysts with 20 and 30 at% Ag show similar differential heat curves and have a $H/Ru_{surface}$ of approximately one at saturation.

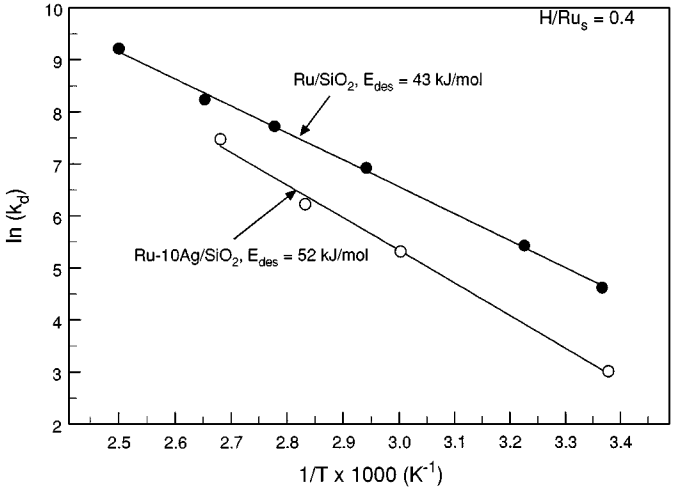

FIG. 3. Arrhenius type plot of exchange parameter versus inverse temperature for Ru/SiO_2 and $Ru{-}10Ag/SiO_2$.

An adsorption energy distribution (Fig. 6) was obtained by counting the number of micromoles of hydrogen adsorbed in a given energy range. The amount of hydrogen adsorbed is normalized by the amount of Ru at the surface, $Ru_{surface}$ (determined from the dispersion measurements). The results in Fig. 6 clearly show that even the $Ru{-}3Ag$ catalyst displayed a perceptible reduction in the amount of intermediate and weak adsorption states.

DISCUSSION

Effect of Ag on Quantity of Chemisorbed Hydrogen

The hydrogen coverages determined in this study were based on 1 : 1 stoichiometry of $H/Ru_{surface}$ under conditions where only strongly bound hydrogen on the metal surface was measured. In a previous study, the experimental conditions were determined such that the 1 : 1 stoichiometry of strong $H/Ru_{surface}$ postulate was valid (15). For all

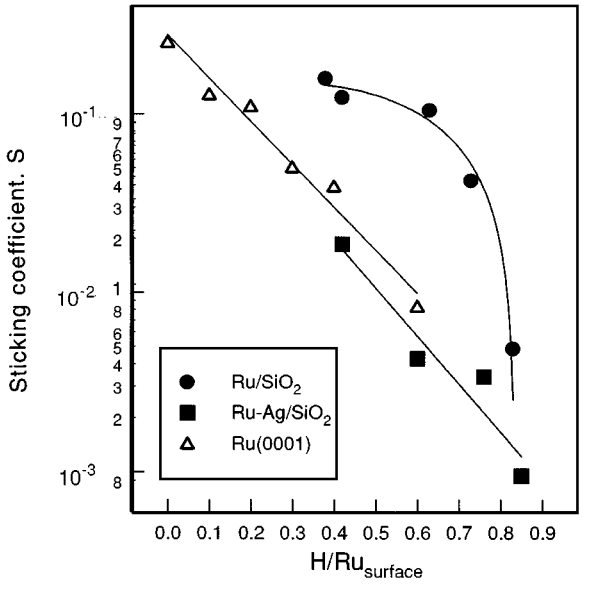

FIG. 4. Apparent sticking coefficient of hydrogen as a function of hydrogen coverage on Ru/SiO_2, $Ru{-}10Ag/SiO_2$, and Ru(0001) catalysts (24).

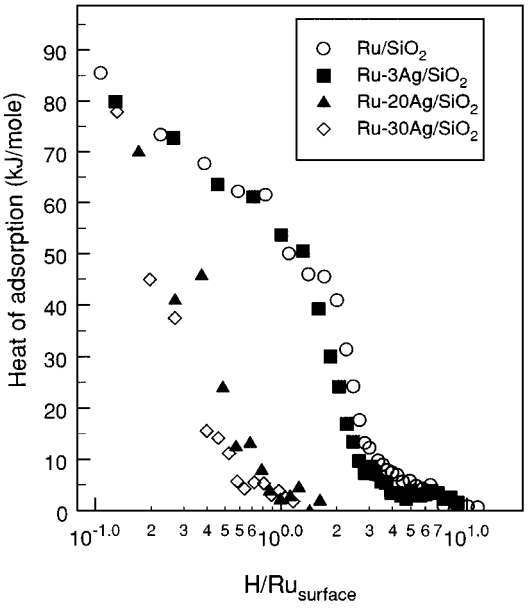

FIG. 5. Heats of adsorption of hydrogen as a function of hydrogen coverage for Ru/SiO_2 and $Ru–3Ag/SiO_2$, $Ru–20Ag/SiO_2$, and $Ru–30Ag/SiO_2$.

the catalysts studied, the surface coverages were based on the surface ruthenium sites accessible for strong hydrogen chemisorption. As the hydrogen pressures increased, the $H/Ru_{surface}$ ratios increased. At high hydrogen pressures, the chemisorbed hydrogen resided in the weakly bound states. These weakly bound states were also confirmed by microcalorimetry data presented in this paper.

At all hydrogen pressures and surface coverages studied in this work the $H/Ru_{surface}$ ratio decreased with increasing Ag content. For example, at 460 Torr H_2 the value of $H/Ru_{surface}$ for Ru/SiO_2 was approximately 3.5, whereas the ratios were 2.5 and 1.5 on $Ru–10Ag/SiO_2$ and $Ru–20Ag/SiO_2$, respectively. Similarly, the respective ratios at 0.4 Torr were 1.1, 0.2, and 0.2. The microcalorimetry results showed that this decreasing hydrogen population was mainly associated with intermediate and low heats of adsorption. Possible reasons for this decrease could be one or more of the following:

(i) silver blocked those Ru sites on the surface where large amounts of hydrogen could be adsorbed;
(ii) an ensemble effect changed the nature of a multiple adsorption site;
(iii) an electronic interaction between Ru and Ag affected the binding of hydrogen to Ru atoms;
(iv) Silver altered the kinetics of hydrogen chemisorption on Ru surfaces.

These points will be discussed in the upcoming sections.

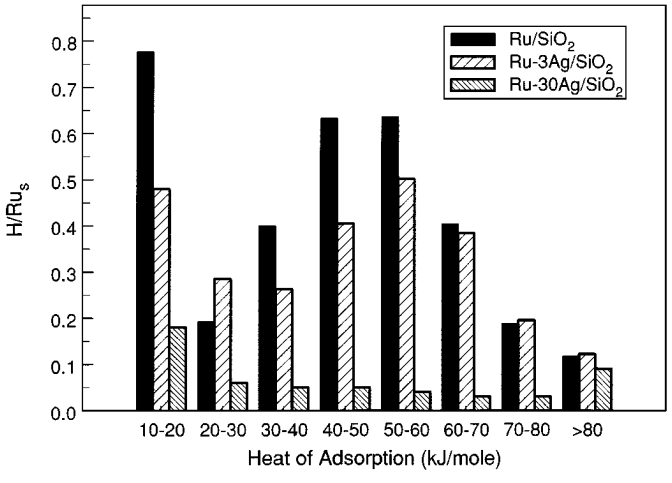

FIG. 6. Adsorption energy distributions for Ru and Ru–Ag bimetallics derived from microcalorimetry results.

Site Blocking and Ensemble Effects

Atomistic simulations of the Ru–Ag system (7, 9) suggested that Ag preferentially occupied the edge, corner, and other low coordination sites. For example, at 30 at% Ag, almost all the edge and corner sites are occupied by silver. Experimental results tend to support this view (11). It may be postulated that the edge, corner, and other low metal coordination surface features of Ru can accommodate additional intermediate and low energy adsorption states of adsorbed hydrogen and that preferential blocking of these sites causes a disproportionate reduction in these states. However, simple site blocking cannot explain the magnitude of the reduction in hydrogen population observed in this work. The low coordination sites occupy only 10–20% of the surface sites for a catalyst with dispersion in the range of 20 to 30%. To account for such a large drop in the overall stoichiometry, each of these edge and corner Ru atoms must accommodate 12 to 20 hydrogen atoms, which seems highly unlikely.

As we already mentioned in the Introduction, it is also unlikely that ensemble effects are present in the Ru–Ag bimetallic system because this system does not exhibit micromixing. Indeed, Ag and Ru do not form bulk alloys because of the severe energy penalty associated with Ru–Ag bonds (7, 9).

Electronic Interactions between Ru and Ag

In this study we observed that the ^1H NMR line shifts of hydrogen on Ru in Ru–Ag catalysts were all essentially the same as those observed on the pure Ru catalyst. The Knight shift, a result of hyperfine interactions of the conduction electrons of Ru metal with the probe nucleus (in our case ^1H), is a measure of the density of the bonding states at the Fermi level. Thus, a lack of change in the Knight shift with increasing amounts of silver indicates that there are no through-metal electronic interactions between Ag and Ru that affect the density of hydrogen–metal bounding states

at the Fermi level. The microcalorimetry results are another indication of this lack of an electronic effect between Ru and Ag, at least as it may influence hydrogen adsorption. Heats of adsorption in the low coverage region are expected to vary if electronic interactions between Ru and Ag are operable. It was observed that the initial, low coverage heats of adsorption of hydrogen are similar for the Ru/SiO_2 and all the $Ru–Ag/SiO_2$ catalysts. As noted earlier the above results are consistent with the XPS and XAES study of Ag on Ru(0001) single crystal surfaces (8).

Effect of Silver on Energetics of Hydrogen Chemisorption

Data presented in Fig. 6 were obtained by counting the number of micromoles of hydrogen adsorbed in a given energy range. The amount of hydrogen adsorbed was normalized by the amount of Ru at the surface, $Ru_{surface}$ (determined from the dispersion measurements). A close examination of Fig. 6 indicates that the $H/Ru_{surface}$ amounts and the energetics associated with the sites that adsorbed hydrogen most strongly (>80 kJ/mol) were influenced little by the presence of Ag. Note that the amount of this strongly bound hydrogen per total mass of Ru does decrease upon addition of Ag (not shown).

One could speculate that these high-energy sites are associated with highly dispersed Ru-rich particles that remain unaffected by the presence of Ag elsewhere on the catalyst, and Ag blocks sites on other particles that adsorb hydrogen with strong and intermediate heats. This is unlikely for two reasons. First, due to the way dispersion is determined these high-energy sites represent a significant fraction of the surface Ru atoms. Furthermore, the catalysts with increasing amounts of Ag have proportionately less of these high-energy sites, but the ratio of the number of these sites to the total number of surface Ru atoms remains essentially the same. Hence, all sites are reduced but the sites with intermediate and strong heats are reduced to a greater extent. Second, if these high-energy sites represent highly dispersed Ru particles, perhaps even monodispersed atoms, then one would expect the ^1H NMR shift observed would vary with Ag content. This would be due to variation of the Fermi level in the particles or even total lack of metallic character for small clusters or isolated Ru atoms. The observed shift would manifest as one peak at higher pressures where the fast exchange limit is operable, or two or more peaks when the hydrogen is relatively immobile. This is not observed. The distribution curves presented in Fig. 6 indicate that the presence of silver influenced the hydrogen populations on intermediate (20 to 60 kJ/mol) and low (<20 kJ/mol) heats of adsorption at low Ag loadings (3%). At 30% Ag loadings, the high-energy sites (60 to 80 kJ/mol) were also lost. But the high-energy sites (>80 kJ/mol) were unaffected even at high loadings of silver.

Effect of Silver on Kinetics of Hydrogen Chemisorption

The adsorption and desorption rate constants presented in Table 2 and the sticking coefficients given in Fig. 4 indicate that Ag dramatically reduces the kinetics of hydrogen adsorption. Two possible explanations of the lowering of the adsorption kinetics by Ag can be considered: (a) Ag inhibits the translational motion of hydrogen on the surface, and/or (b) the sites blocked by Ag are the most active for dissociative hydrogen adsorption. These points are discussed below.

(a) If Ag restricts the translational motion of hydrogen molecules parallel to the Ru surface, then the molecule may not have sufficient residence time on the surface to be "trapped" (24). Since Ag does not accommodate hydrogen, adsorbing hydrogen molecules would likely desorb rather than pass over Ag sites. The adsorbed molecule is thought of as a precursor state in this proposed mechanism and Ag reduces the likelihood that the precursor can move into a chemisorbed state. However, this mechanism for reduction in rates of hydrogen adsorption seems unlikely for the same reasons as discussed for the possibility of ensemble effects. The clustering nature of Ag in a Ru environment is too high and regions of large Ru ensembles must exist on the catalyst even at high Ag contents.

(b) It is known from studies on single crystals that hydrogen may dissociate and adsorb more rapidly on defect-like sites than on extended low index planes. For example, Bernasek and Somorjai (25) reported that stepped Pt(997) and Pt(553) surfaces were approximately 100 times more active for hydrogen–deuterium exchange than Pt(111). Similarly, Smith *et al*. (26) proposed that the edge sites are more active for dissociative adsorption of hydrogen on supported Pt and Pd catalysts. The earlier atomistic simulations (7, 9) and the kinetic data derived here from selective ^1H NMR are consistent with these observations. That is, by blocking edge and corner sites, Ag lowered the kinetics of hydrogen adsorption on Ru–Ag bimetallic particles relative to pure Ru particles. Indeed, the sticking coefficient of hydrogen on the Ru–Ag particles given in Fig. 4 is similar to that on a defect-free Ru(0001) single crystal (23). The reason is that once all edge, corner, and other low coordination sites are populated, all Ru at the surface is in low index plane facets.

The term coined for this rapid, site-specific or surface-sensitive adsorption is "portal"-mediated adsorption. It is likely that this process is zero order in hydrogen pressure and initially produces weakly bound, highly mobile hydrogen that migrates to unfilled, strong binding sites. Indeed, this "portal"-mediated process is consistent with the lack of coverage dependence of the apparent sticking coefficient at lower coverages on Ru catalyst noted in Fig. 4 (27). Likewise, the desorption process requires two hydrogen atoms combining to form the desorbing molecule. The two atoms

may be both strongly adsorbed (SS), both weakly adsorbed (WW), or a combination of weakly and strongly adsorbed species (WS). The relative rates of the elementary desorption processes should be WW > WS > SS based solely on the energy barriers.

When the portals are systematically closed, for example, by allowing Ag to distribute to edges and corners, the elementary adsorption process at those sites is shut down, but the desorption process still can occur to the extent that the populations of surface hydrogen exist. Note that adsorption directly onto basal plane-like facets still occurs at its intrinsically slower rate (25, 26). Hence, the qualitative picture that emerges is that the weakly bound states are systematically depopulated due to a reduced adsorption rate coupled with desorption favoring the more weakly bounds states. The net result is a surface with less total hydrogen and an adsorption energy distribution more heavily weighted to the higher energy states. The calorimetry results (Figs. 5 and 6) and the adsorption isotherms (Fig. 2) found in this study are consistent with this model.

Note that in this picture, microscopic detailed balance is not achieved especially at higher pressures where weakly bound states exist and spillover to the support is facile. Hence, the calorimetry results are not truly at equilibrium under these conditions. Rather, these experiments probe a stationary state. However, one has to note that the calorimetry experiments are performed under such conditions that the spilled over hydrogen was mobile enough such that the desorption process from the support surface was also facile (15).

Additional evidence indicating that the adsorption/desorption operation does not follow a simple mechanism such as a Langmuir process is given in Table 2. For example, the values of the rate constants for desorption for the two catalysts are a strong function of coverage, while the rate constants for adsorption do not vary much with coverage.

The portal mediated adsorption model outlined above can explain catalytic variations previously observed for some bimetallic systems. For example, Smale and King (7) noted that even though Ag is catalytically inert, does not adsorb hydrogen, and cannot produce an ensemble effect, it can significantly alter the ethane hydrogenolysis reaction on Ru. Ru–Ag catalysts yielded a significantly more negative order of reaction with respect to hydrogen on Ru–Ag compared to Ru catalysts, −2.5 versus −1.5. Smale and King (7) postulated a simple mechanism, where the hydrogen and ethane adsorption processes were at equilibrium and the rate determining step was that of fragmenting the adsorbed ethane molecule to surface intermediates step. Based on this model the ethane hydrogenolysis reaction rate law took the form

$$\text{Rate} = \frac{kK_E P_E}{(K_H P_H)^{n/2}\left(1 + (K_H P_H)^{1/2}\right)^2}, \qquad [1]$$

where K_E is the equilibrium constant for ethane adsorption step, K_H is the equilibrium constant for hydrogen adsorption step, P_E is the partial pressure of ethane, P_H is the partial pressure of hydrogen, k is the rate constant of the rate determining step, and n is the number of hydrogen atoms that must be removed from the adsorbing ethane in an equilibrated adsorption step.

Based on the model explained above and the resulting rate law, the authors concluded that the net effect of Ag on ethane hydrogenolysis was lowering the rates of desorption of hydrogen. This postulate was confirmed with the present evidence collected from NMR spectroscopy: data presented in Table 2 indicate that the desorption rate constant of hydrogen has decreased by about an order of magnitude upon introduction of Ag to a Ru/SiO_2 catalyst. Lower rates of desorption of hydrogen would result in a larger effective value of K_H in the model described above (7). Larger effective value of K_H results in larger average heats of adsorption of hydrogen in the presence of Ag on Ru. The results presented here reveal that the average heat of adsorption is indeed higher on the Ru–Ag bimetallic catalysts than on the pure Ru catalyst.

CONCLUSIONS

In this paper we report a study to determine the amounts, dynamics, and energetics of hydrogen chemisorption on silica supported ruthenium and ruthenium-silver bimetallic catalysts. This work employed a unique combination of ^{1}H NMR spectroscopy and microcalorimetry. The NMR is used to determine the amount of hydrogen adsorbed on the Ru surface quantitatively and to determine the kinetics of the adsorption and desorption processes. We find that on $Ru–Ag/SiO_2$ the amount of hydrogen adsorbed per surface Ru atom is less than in the Ru/SiO_2 system. Also, from microcalorimetry, the populations of low and intermediate energy binding states of hydrogen are found to be lower on Ru–Ag catalysts. The rate constants for hydrogen adsorption and desorption, determined from selective excitation ^{1}H NMR, are 20 to 100 times lower on $Ru–Ag/SiO_2$ compared to Ru/SiO_2 at a given hydrogen coverage. The apparent sticking coefficients of hydrogen were at least tenfold lower on Ru–Ag catalyst (10 at% Ag) than those on the Ru catalyst at the same temperature and hydrogen coverage. The ^{1}H NMR Knight shifts of adsorbed hydrogen and the initial heats of hydrogen adsorption are essentially the same on Ru/SiO_2 and on all $Ru–Ag/SiO_2$ catalysts.

The similarity of initial heats of adsorption and ^{1}H Knight shifts strongly indicate that Ag does not effect the electronic state of the H–Ru interaction. Furthermore, ensemble effects are ruled out for this bimetallic system because of its inability to produce any significant degree of micromixing on the surface. It is proposed that the influence of Ag on the hydrogen adsorption, both rates and amounts, is generated

by structure sensitive hydrogen adsorption, i.e., blocking of edge, corner, and other low metal coordination sites by silver altering the hydrogen chemisorption rates. The hypothesis is based on the understanding that low coordination (edge and corner) sites are significantly more active for dissociative adsorption of hydrogen.

ACKNOWLEDGMENTS

This work was supported by the U.S. Department of Energy, Office of Basic Energy Sciences, Division of Chemical Sciences, under Contract W-7405-ENG-82, and by the National Science Foundation, Engineering Research Equipment Grant CBT-8507418.

REFERENCES

1. Sinfelt, J. H., "Bimetallic Catalysts," Wiley, New York, 1983.
2. Clarke, J. K. A., *Chem. Rev.* **75**, 291 (1975).
3. Ponec, V., *Adv. Catal.* **32**, 149 (1983).
4. Sachtler, W. M. H., and van Santen, R. A., *Adv. Catal.* **26**, 69 (1977).
5. Chuang, S. S., and Pien, S.-I., *J. Catal.* **138**, 536 (1992).
6. Chuang, S. S., Pien, S.-I., and Narayanan, R., *Appl. Catal.* **57**, 241 (1990).
7. Smale, M. W., and King, T. S., *J. Catal.* **120**, 335 (1990).
8. Rodriguez, J., *Surf. Sci.* **296**, 149 (1993).
9. Strohl, J. K., and King, T. S., *J. Catal.* **116**, 540 (1989).
10. Wu, X., Gerstein, B. C., and King, T. S., *J. Catal.* **123**, 43 (1990).
11. Schick, M., Ceballos, G., Pelzer, Th., Rangelov, G., Stober, J., and Wandelt, K., *Surf. Sci.* **307**, 582 (1994).
12. Engelke, F., Vincent, R., King, T. S., and Pruski, M., *J. Chem. Phys.* **101**(9), 7262 (1994).
13. Hayward, D. O., and Tarpnell, B. M., "Chemisorption," 2nd ed., pp. 75, 233, Butterworths, Washington, DC, 1964.
14. Wu, X., Gerstein, B. C., and King, T. S., *J. Catal.* **121**, 271 (1990).
15. Uner, D. O., Pruski, M., and King, T. S., *J. Catal.* **156**, 60 (1995).
16. Narayan, R. L., and King, T. S., *Thermochim. Acta* **312**, 105 (1998).
17. Handy, B. E., Sharma, S. B., Spiewak, B. E., and Dumesic, J. A., *Meas. Sci. Technol.* **4**, 1350 (1993).
18. Cardona-Martinez, N., and Dumesic, J. A., *Adv. Catal.* **38**, 149 (1992).
19. Robell, A. J., Ballou, E. V., and Boudart, M., *J. Phys. Chem.* **68**, 2748 (1964).
20. Miller, J. T., Meyers, B. L., Modica, F. S., Lane, G. S., Vaarkamp, M., and Konnigsberger, D. C., *J. Catal.* **143**, 395 (1993).
21. Hwang, S.-J., Uner, D. O., King, T. S., Pruski, M., and Gerstein, B. C., *J. Phys. Chem.* **99**, 3697 (1995).
22. Savargaonkar, N., Ph.D. dissertation, Iowa State University, 1996.
23. Shimizu, H., Christmann, K., and Ertl, G., *J. Catal.* **61**, 412 (1980).
24. Xu, C., and Koel, B. E., *J. Chem. Phys.* **100**(1), 664 (1994).
25. Bernasek, S. L., and Somorjai, G. A., *J. Chem. Phys.* **62**(8), 3149 (1975).
26. Smith, G. V., Bartòk, M., Nothseiz, F., Zsigmond, A. G., and Pàlinkò, I., *J. Catal.* **110**, 203 (1988).
27. Morris, M. A., Bowker, M., and King, D. A., *in* "Comprehensive Chemical Kinetics" (C. H. Bamford, C. F. H. Tipper, and R. G. Compton, Eds.), Vol. 19, p. 1. 1984.